KHARIF RICE CROP ACREAGE AND YIELD ESTIMATION USING MICROWAVE AND OPTICAL REMOTE SENSING TIME SERIES SATELLITE DATA: A CASE STUDY OF THE EASTERN REGION OF MAHARASHTRA

Pritam Meshram 0000-0003-1555-2644, Kishan Singh Rawat✉ 0000-0001-5900-8195, Gaurav Singh 0000-0002-6469-828X

Geo-Informatics, Department of Civil Engineering, Graphic Era (Deemed to be University) (Accredited with Grade 'A+' by NAAC), 248002 Dehradun, Uttrakhand, India

ABSTRACT

Aim of the study
The study aims to assess the feasibility of using remote sensing to estimate crop area and yield in a major rice-growing region of Maharashtra.

Material and methods
Recent advancements in remote sensing technology, including improvements in image resolution and availability, allowed for timely data collection. The study employs a random forest classifier to identify rice crop using sentinel-1A SAR temporal backscatter satellite images. Additionally, a semi-physical method that incorporates remote sensing and physiological concepts such as Photo-synthetically Active Radiation and a fraction of PAR absorbed by the crop is used to estimate crop yield.

Results and conclusions
Net Primary Product was calculated using the Monteith model. The calculation of Kharif rice yield involved considering the actual NPP, Radiation use efficiency, and Harvest index. The present study was conducted throughout two kharif seasons, 2020 and 2021. Although there are minor differences in kharif rice area and yield estimations, the model is still applicable in other significant kharif rice-growing regions of India.

Keywords: remote sensing, SAR, backscatter, MODIS, fAPAR, NPP, LSWI, temperature

INTRODUCTION

With 70% of the workforce employed in agriculture and contributing roughly 30% of the GDP, India's economy is based primarily on this sector. Estimating crop production ahead of harvest is extremely useful in farming for purposes such as implementing appropriate agricultural management and pricing agricultural commodities for export/import. Calculating the total area covered by the crop and projecting the yield for each unit area are necessary steps in the assessment of crop production. Crop acreage and yield estimation are required because they play an important role in the national economy; in planning food security for a district/population; in the country, in warning decision-makers about potential crop yield reductions; in

✉e-mail: ksr.kishan@gmail.com

allowing timely import and export decisions; and in assisting private companies in planning supply chain decisions such as production scheduling. The accuracy and speed of crop yield estimation influence agricultural-economic and yield price policy (Tikkiwal and Khandelwal, 2012; Kosmowski et al., 2021). In many nations, agricultural yield estimation is based on conventional methods of gathering data for crop and yield estimation, such as field visits & reports. These reports are frequently subjective and take more time and money to complete. In many nations, agricultural yield estimation is based on conventional methods of gathering data for crop and yield estimation, such as field visits and reports (Bhattacharya et al., 2020; Gummadi et al., 2022). Remote sensing techniques have shown promise in giving information on the features and spatial distribution of natural resources, particularly agricultural resources, due to their unique ability to give multi-spectral, multi-temporal, and multi-spatial resolutions (Lin et al., 2022). Compared to conventional ground-based agricultural resource assessments, satellite remote sensing data has shown to be more economical, dependable, timely, and fast. In order to identify and track crop growth and predict crop output, remote sensing spectral reflectance data is a manifestation of the combined influence of weather, soil, cultural methods, and crop features (Kumar et al., 2021; Torre et al., 2021; Safdary et al., 2022). Further, it addresses some Sustainable Development Goals (SDG) such as SDG 1 (no poverty), SDG 2 (zero hunger), and SDG 15 (life on land) (UN, 2021).

Strategic decision-making requires timely and accurate crop area and yield data, which is widely understood by all parties involved in agriculture, including farmers, processors, resource managers, marketers, financiers, and the government. It is essential to keep an eye on the rice farming sector in order to obtain data that would help food security strategy. With the use of remote sensing data, it is possible to quickly, accurately, and efficiently estimate crop identification, monitoring, acreage, and yields. Using input from MODIS satellite data and the Temperature Vegetation Dryness Index (TVDI), the triangular network approach can map the soil moisture, which is necessary for high agricultural output. The results demonstrate a substantial correlation between in-situ soil moisture. Several crops have been identified using optical remote sensing on a large scale. However, because of the dark and rainy conditions during the kharif season, optical pictures are frequently unavailable during the critical growing stage of the crops. This has a negative effect on agricultural area monitoring's accuracy and timeliness. A unique method that has been widely employed in agriculture to track and detect crop status is Synthetic Aperture Radar (SAR). Its advantages include comprehensive coverage, good resolution, day-and-night collection, and weather independence.

India is one of the few nations with a systematic approach in place for gathering agricultural statistics, dating back to 1884. The area under crop and the average yield per unit area are often multiplied to determine the agricultural crop production of the nation's primary crops. District-level crop acreage estimates are achieved by comprehensive enumeration, whereas general crop estimating surveys (GCES) based on crop-cutting experiments carried out on several randomly selected fields in a sample of the district's villages produce the average yield. The Ministry of Agriculture currently creates crop predictions and advanced estimations of crops. Unfortunately, the subjective, costly, time-consuming, labour-intensive, and error-prone nature of these reports can lead to inaccurate estimates of crop area and yield. Furthermore, data on crop acreage and yield arrive late in most states, making it difficult to assess, draw conclusions, and take the necessary action to prevent food shortages. Since the 1970s, remote sensing technology has been used all around the world for crop identification, monitoring, and production forecasting, as well as for acreage under cultivation. There are now many methods developed for early crop yield estimation based on remote sensing data (RSD). The primary data sets utilised for this purpose are those with moderate spatial resolution (MODIS) and low spatial resolution (NOAA, MSG, VHRR, SPOT VEGETATION), which enable the acquisition of up-to-date information on the condition of crops with high economic efficiency (Klisch et al., 2006).

However, rather than providing an actual crop yield, this approach just provides a prospective yield. While water stress and nitrogen shortage (Sinclair and Horie, 1989) have an impact on radiation conversion efficiency, temperature stress and water stress during

the reproductive and grain-filling phases have an impact on the harvest index. The goal of the current study was to use remotely sensed SAR data and the Monteith equation to predict rice crop production at the district level.

METHODOLOGY

Study area

Bhandara district in Maharashtra (see: Figure 1), referred to as the 'RICE BOWL' of the state, is a major rice-producing region in Vidarbha. Covering an area of 3716 square kilometres, it shares its border with Nagpur. With an average temperature of 27.1 degrees centigrade, the district receives a significant amount of rainfall, ranging between 1200–1300 mm annually, which is the highest in Vidarbha. The region benefits from two main rivers, the Wainganga and Surnadi, providing irrigation resources for rain-fed and irrigated agriculture. Canals, wells, and tanks ensure proper watering of agricultural lands. The district's soil is classified into the categories of deep soil (78.9%), shallow soil (13%), and moderately deep soil (8%), allowing for the cultivation of a wide range of crops and enhancing agricultural productivity.

Crop classification

Rice has specific temporal characteristics, and we rely on the link between the backscatter or intensity of the signal reflected back to the SAR sensor and how it
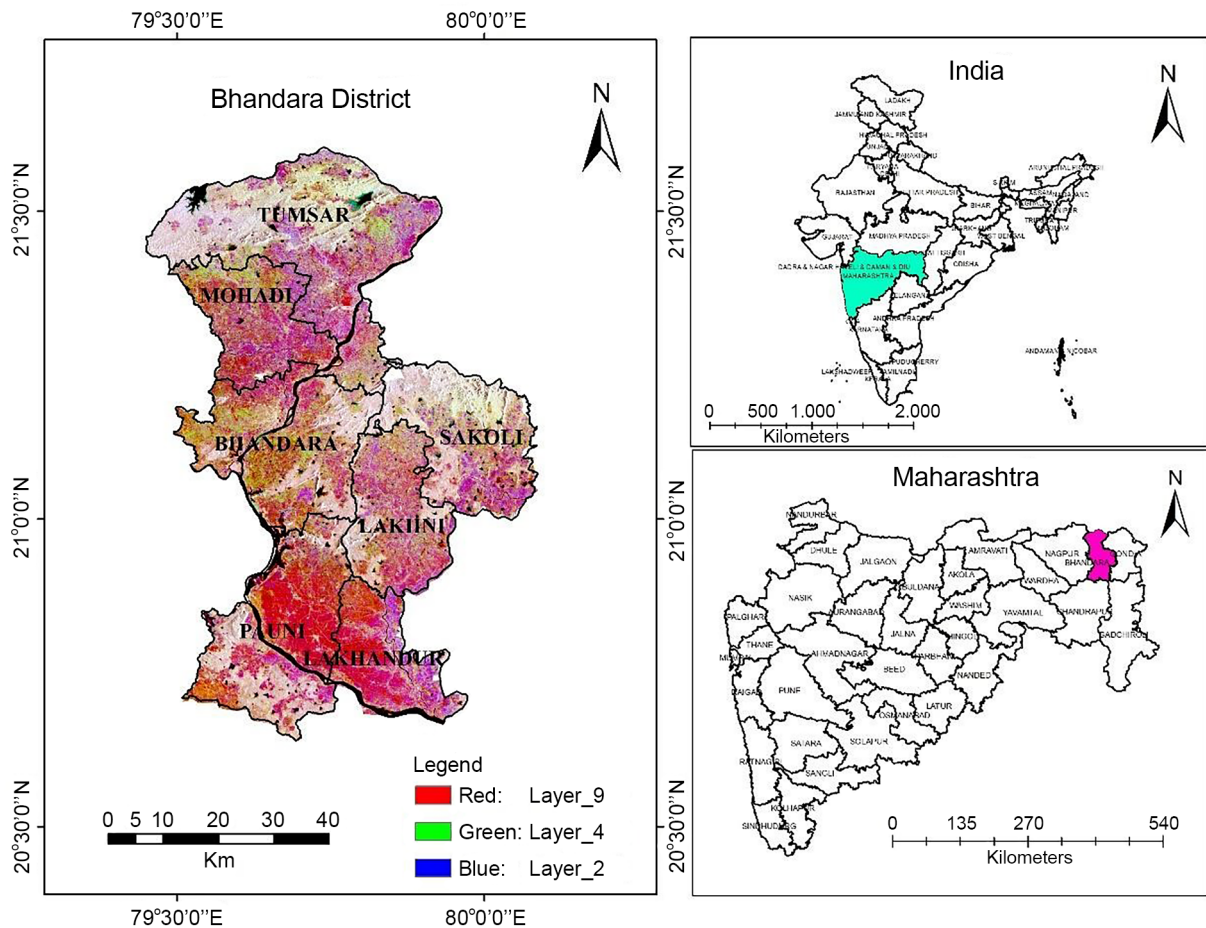

Fig. 1. Area of interest located in the region of eastern Maharashtra (Bhandara district, Maharashtra) (source: Authors' own elaboration)

changes over time to monitor and map rice. Because the soils are inundated with water, backscatter during land preparation is minimal in the C-band. Due to the increased height, biomass, and density of the crop, there is a corresponding rise in backscatter, which increases the backscatter signal. When biomass, height, and density do not significantly alter during the reproductive phase, the backscatter remains constant.

We obtained Sentinel-1 SAR images (VH polarisation) during mid-June to November for the kharif rice growing season in 2020 and 2021 from Google Earth Engine. These images had a spatial resolution of 10 meters, and a revisit after 12 days (Table 1). The Sentinel-1 SAR images were pre-processed before being analysed, which included orbital correction, thermal noise reduction, speckle filtering, radiometric calibration, and range-doppler terrain correction. The Sentinel Application Platform (SNAP) software from the European Space Agency (ESA) was used in these

processes, as detailed by Schubert et al. (2015) and Valcarce-Diñeiro et al. (2019).

For supervised classification using remote sensing datasets, a Random Forest classifier (RF) was used since it performs better than other machine learning algorithms (Ma et al., 2017; Belgiu and Csillik, 2018; Silveira et al., 2019). Stack satellite image and training samples, which included paddy, waterbodies, settlements, forests, and other crops, were imported in the SNAP software, then the number of trees (25) was set; following that, all bands in the stack will be used for the training of the classifier. When you have bands that you cannot use for training, this is crucial. Now, the Random Forest classifier (see: Figure 2) pulls every pixel beneath the training polygons and searches for thresholds that, as much as feasible, allow the separation of the various input types. The ultimate outcome is significantly influenced by the calibre of the training data.
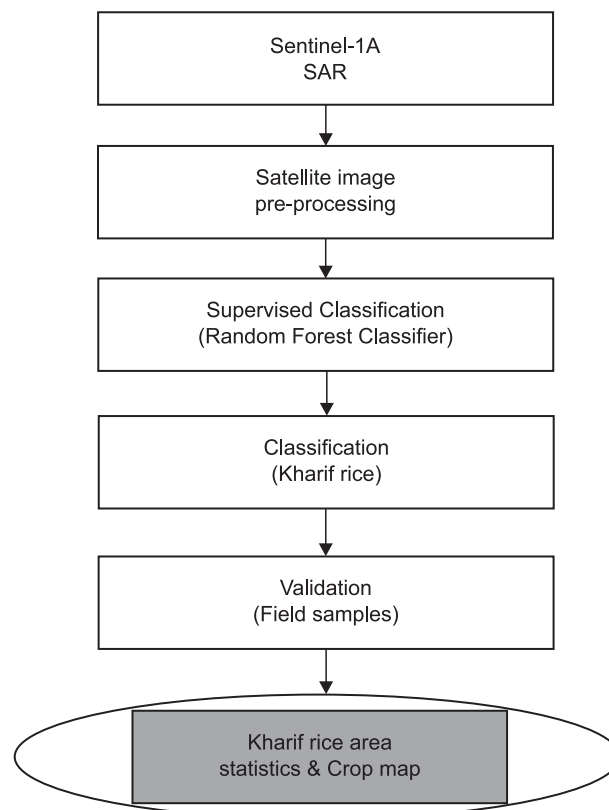

Fig. 2. Flow chart of crop classification (source: Authors' own elaboration)

Table 1. Information of SAR Dataset (source: Authors' own elaboration)

Datasets	Microwave SAR Data
Source	Sentinel-1 SAR GRD (VH)
Period	June-November (Kharif 2020, 2021)
Spatial resolution	10 m
Temporal resolution	12 days
Pre-processing	Radiometric correction, Speckle filter, Terrain correction

Yield Estimation

The yield prediction system is based on tracking the daily growth in plant biomass from the beginning of the growing season to the maturity stage. The idea is that plant growth may be impacted by incoming solar radiation, namely by the quantity of photosynthetically active radiation (PAR) received, and the crop's ability to intercept PAR. Monteith (1977) developed the formula to measure the fAPAR. The ratio of incident PAR to absorbed PAR is known as fAPAR (0 < fAPAR < 1). The total intercepted photo-synthetically active radiation is known as PAR (see: Figure 3). The formula below can be used to estimate photosynthetic active radiation.

$$PAR = Rs \times 0.5 \qquad \text{eq. (1)}$$

The rice biomass accumulation model can be expressed in a general manner as follows:

$$NPP = fAPAR \times PAR \times RUE \qquad \text{eq. (2)}$$

where:
PAR – photosynthetically active radiation ($MJm^{-2} d^{-1}$),
RUE – radiation-use efficiency of absorbed photosynthetically active radiation (gMJ^{-1}),
$fAPAR$ – fraction of incident PAR that is intercepted as well as absorbed by the canopy (dimensionless),
NPP – net primary productivity/dry matter accumulation in the plant over a period of time ($gm^{-2} d^{-1}$).

Radiation use efficiency (RUE) is described as:

$$RUE(gMJ^{-1}) = Biomass \text{ } (g/m^2) \text{ } / \text{ } PAR(MJ/m^2/day)$$
$$\text{eq. (3)}$$

where:
Rs – incoming solar radiation (MJm^{-2}).

Since observations have also been made about the effects of temperature stress (T_{stress}) and water stress (W_{stress}) on photosynthesis, the revised equation becomes:

$$NPP = fAPAR \times PAR \times RUE \times W_{stress} \times T_{stress} \qquad \text{eq. (4)}$$

The product of the net primary productivity (NPP) and the harvest index (HI) yields the economic grain yield. That is:

$$Grain \text{ } Yield = \sum_{Sowing}^{Harvesting} NPP \times HI \qquad \text{eq. (5)}$$

Where the following formula is used to determine the Harvest Index (HI) from supplementary CCE data:

$$HI = Grain \text{ } Yield \text{ (Kg/ha)} / Biomass \text{ Yield (Kg/ha)}$$
$$\text{eq. (6)}$$

Field survey

Field survey data is essential for analysing remote sensing data and distinguishing various land uses and land cover. The ground data was collected using MAP-Inr, an Android smartphone app. This application uses polygons to mark the field. During a field survey, basic information collected in tabular form includes crop type, GPS coordinates (Latitude and Longitude), field dimensions, crop health, crop stage, images, ground cover, planting date, anticipated harvest date, and soil quality. Data from field surveys were collected during July, August, and September.
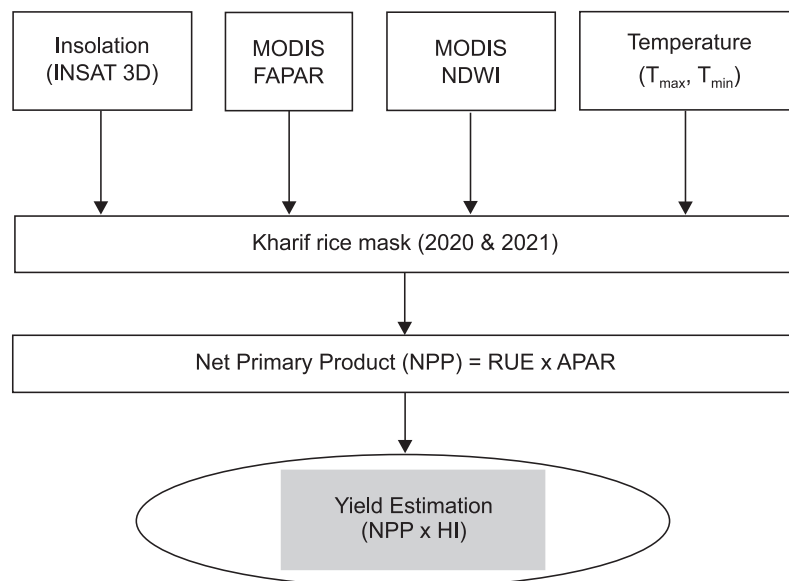
Fig. 3. Flow chart of yield estimation (source: Authors' own elaboration)

Table 2. Datasets used in study (source: Authors' own elaboration)

Sr. No.	Data	Satellite	Sensor	Resolution	Source
1	Daily integrated insolation	INSAT 3D	Imager	1 km	www.mosdac.gov.in
2	8 days composite FAPAR	Terra	MODIS	0.5 km	LPDAAC@usgs.gov
3	8 days composite surface reflectance	Terra	MODIS	0.5 km	LPDAAC@usgs.gov
4	Daily Tmin and Tmax	Ground station of IMD		0.5×0.5 degree	IMD, Pune data
5	RUE, Harvest Index				Old literature and Review

Rainfall

Rainfall during the monsoon season is crucial for rice plant sowing, an important step in growing rice. An adequate water supply is needed for the young paddy seedlings to thrive. Farmers determine the best time for transplantation by monitoring local weather patterns and forecasts. Insufficient rainfall can lead to delayed planting and hinder seedling growth, while excessive rainfall can result in flooding and complicate paddy plant transplantation. Therefore, a balanced and timely distribution of rainfall is necessary for successful paddy crop establishment.

The rainfall during the kharif rice growing season is depicted in Figure 4 (maharain.maharashtra.gov.in). The district experienced more rainfall in June and July than usual, which is beneficial for the growth of rice nurseries. August rainfall was above average in 2020 and below average in 2021, affecting the crop plant development stage and resulting in a reduction in productivity.
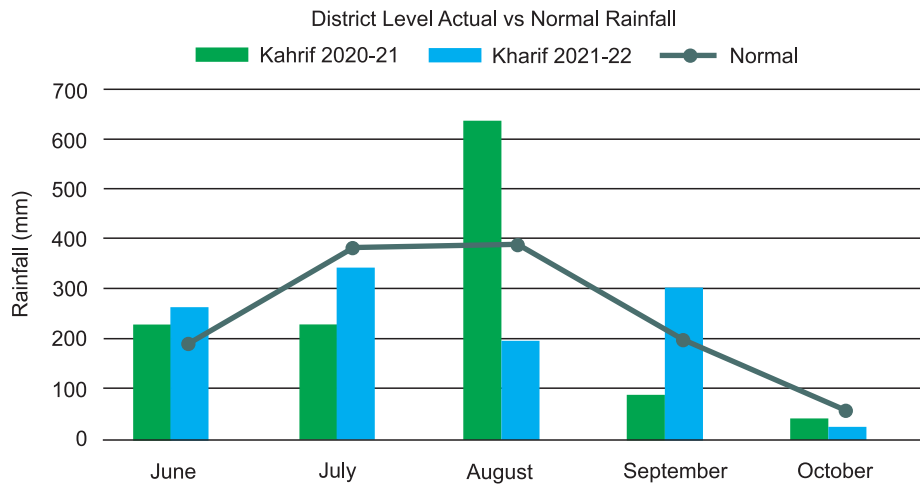
Fig. 4. Rainfall Distribution (Rainfall during kharif rice growing period) (source: maharain.maharashtra.gov.in)

RESULTS AND DISCUSSION

Crop Classification

A study was carried out to investigate how correctly paddy planting areas could be detected and mapped during two consecutive kharif rice seasons (2020 and 2021), using VH polarization (C band) Synthetic Aperture Radar (SAR). The study utilized SAR backscatter data from June to November, covering the entire crop period and including various types of paddy crop varieties. The paddy crop profile in Figure 5 has been generated using sentinel-1 SAR data. In order to identify the paddy pixels on the satellite image and develop the phenology of the paddy crop, field survey samples were gathered and overlaid. Throughout the district, we noticed various varieties of paddy and the variations in sowing times.

The intensity of VH backscatter in rice crops gradually increased after transplanting. Backscatter intensities in the study region rice fields ranged from –26 to –24 dB during the sowing phase and from –14 to –15 dB during the heading stage (around 65 days after transplanting). During the sowing season, a high-density rice field is directly planted into flooded soil with a depth of 2–5 cm of water. It also results in fairly low VH backscatter intensities, which could be attributed to the cross-polarization of the VH backscatter, which occurs when the waves partially depolarized.
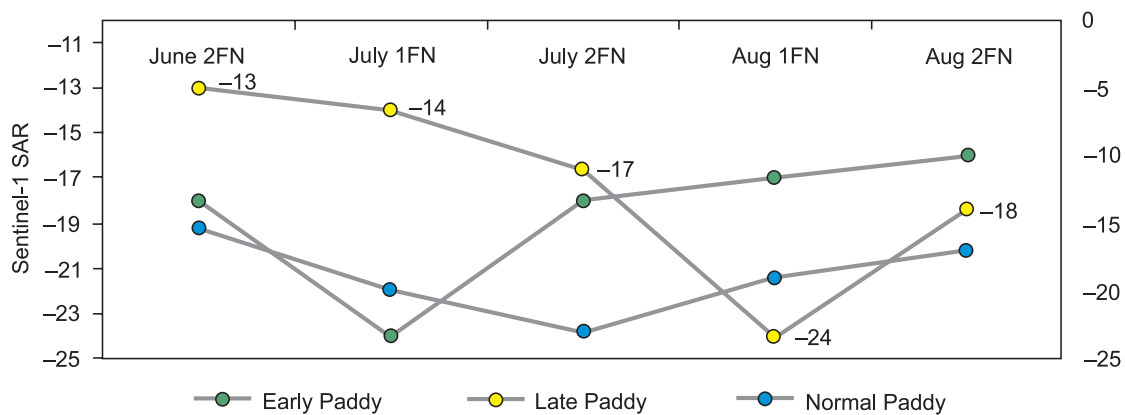

Fig. 5. Sentinel-1 SAR backscatter kharif rice profile (Early, Late and Normal) (source: Authors' own elaboration)

The Random Forest classifier (RF) was utilised and showed superior performance compared to other supervised machine learning algorithms for remote sensing information. To train the classifier, ground truth dataset was used to identify paddy crop areas in satellite images, which were labelled as "paddy" and "non-paddy". The classifier was trained to recognize and classify similar features in the images. The random forest technique combines multiple decision trees to predict outcomes and classify all pixels in the satellite image. This classification was used to create a map (see: Figure 6) showing the spatial distribution of paddy crops in the study area. To further assess the validity of the rice maps derived from Sentinel-1 SAR data, we calculated rice area at the district level and compared the estimates to the official data published by Maharashtra's Department of Agriculture. We found variation in the district's paddy area, ranging from –1.80% to –2%. For the years 2020 and 2021, the overall kharif rice classification accuracy was found to be 83% and 86%, respectively. This high level of accuracy is impressive, especially considering the challenges associated with SAR data interpretation, such as noise and the complex scattering mechanisms of crops. The reported variation in district paddy area (–1.80% to –2%) is minimal, indicating high consistency. Similar studies have shown variations ranging from –5% to +5%, suggesting that the present approach is more precise. Monitoring crop acreage over multiple years, as it has been done (2020 and 2021), provides insights into the stability and reliability of the method. Studies that conduct multi-year analyses often report increased confidence in their methodologies, with year-to-year variations providing a measure of the method's robustness.

The findings imply that the study location has seen consistent outcomes from the use of multi-temporal Sentinel-1 SAR dataset for mapping rice areas. Comparable research, such as the mapping of rice-growing regions in the Mekong Delta in the spring of 2015––2016, produced an 85.3% classification accuracy using a decision tree approach.

In Sahibganj district, Jharkhand, India, the estimation of paddy acreage using Sentinel-1 data and an RF classifier produced an overall accuracy of 90% for the study. In a further study, the spatial distribution of paddy rice fields was mapped using an RF classifier in the Sanjiang plain of northeastern China using multi-temporal Sentinel-1A SAR data (VH polarisation) and Landsat-derived normalised difference vegetation index (NDVI) dataset. The overall categorization accuracy for paddy rice produced by this study was 96.7%. An investigation that used multitemporal Sentinel-1A data with an RF classifier to map the systems of rice cultivation in the South Vietnamese provinces of An Giang & Dong Thap, produced an overall accuracy of 86.1%. The current study produced a decent classification accuracy for India's tropical semiarid conditions when compared to the previously mentioned studies (Subbarao et al., 2020).

Other studies utilizing SAR data for agricultural monitoring often report classification accuracies ranging from 75% to 90%. For instance, a study using Sentinel-1 SAR data for crop classification in European regions reported accuracies around 80-85%. In this research, 83% and 86% accuracies are consistent with the upper range of these results, indicating a well-optimized classifier and effective preprocessing steps.

Yield Estimation

Rice yield from sowing to harvest was measured at 8-day intervals between June 15 and October 30, in the district. This period was identified as the kharif rice crop season based on field survey data and the Sentinel-1 SAR backscatter profile. Figure 5 shows the transplantation dates of the rice plants, indicating that sowing occurs from mid-June to the first half of August. There is an increase in crop greenness from the August to the end of mid-September which depends on the crop sowing varieties. Water stress was applied until the panicle initiation stage of crop growth. The highest water stress was observed in the month of August 2022, while in 2020, water stress ranged from 0.82 to 1 on a scale of 0–1, where 0 represents maximum stress & 1 represents no stress.

During the growing season, Net Primary Product (NPP) was computed using the state's primary cultivar's maximum radiation usage efficiency, every eight days. By calculating composite photo-synthetically active radiation (PAR) and fAPAR every eight days, the periodically absorbed photo-synthetically active radiation (APAR) was measured. This data was integrated for the entire crop season using a kharif rice crop mask. The harvest index of the relevant cultivar
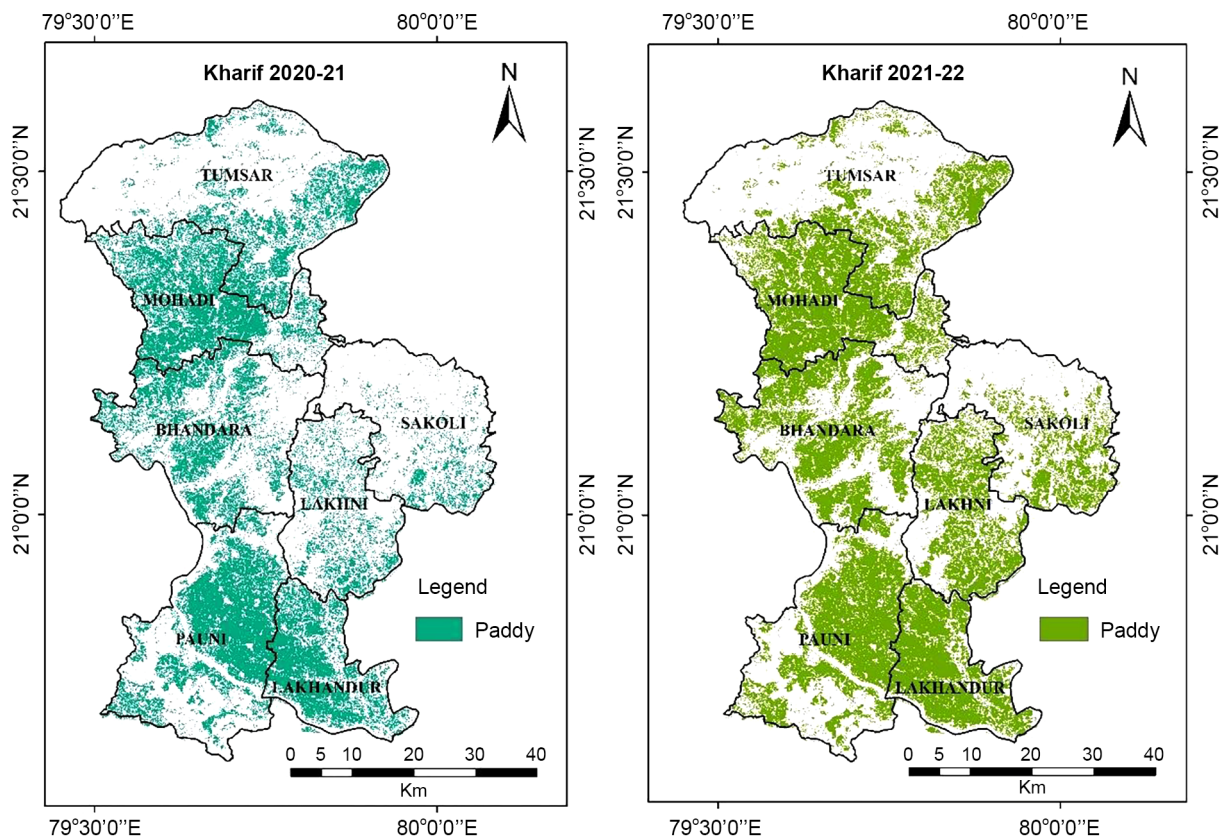
Fig. 6. Kharif rice classification map (2020–2021 and 2021–2022) (source: Authors' own elaboration)

in the state, which varied from 1.5 to 1.8, was used to calculate the grain yield from the total NPP. The district-estimated grain yield ranged from 1500 kg/ha to 2400 kg/ha, as shown by the dispersed yield map (see: Figure 7), which displayed areas of high and low yield. The district-level evaluated average yield was compared to official statistics released by Maharashtra's Department of Agriculture. The kharif rice yield varied by +7.91% and +10.16% for the years 2020 and 2021, respectively. These variations suggest that the estimated yields are slightly higher than the official statistics, which could be due to several factors including local conditions such as soil quality, water availability, and climatic factors.

The estimated yield range (1500–2400 kg/ha) is consistent with other regional studies on rice yield. For example, a study in India using MODIS data and agro-meteorological models reported yield ranges from 1200 kg/ha to 2600 kg/ha, depending on the

region and the year. The yield variation of +7.91% (2020) and +10.16% (2021) indicates that the model tends to slightly overestimate yields compared to official statistics. This level of deviation is comparable to other remote sensing-based studies, which typically report yield prediction errors ranging from 5% to 15%.

Similar studies often employ remote sensing data and vegetation indices (e.g., NDVI, EVI) alongside meteorological data to estimate crop yields. For instance, studies using MODIS-derived vegetation indices coupled with climate data have reported yield prediction accuracies within 10–15% of actual yields. The use of 8-day composite products incorporates temporal fluctuations, yielding a more dynamic and flexible model than static or single-date observations. NPP and fAPAR are important measures of plant productivity and health. Studies that include these parameters frequently obtain greater accuracy in yield forecasts. For example, research in China that used NPP and fAPAR revealed yield esti-
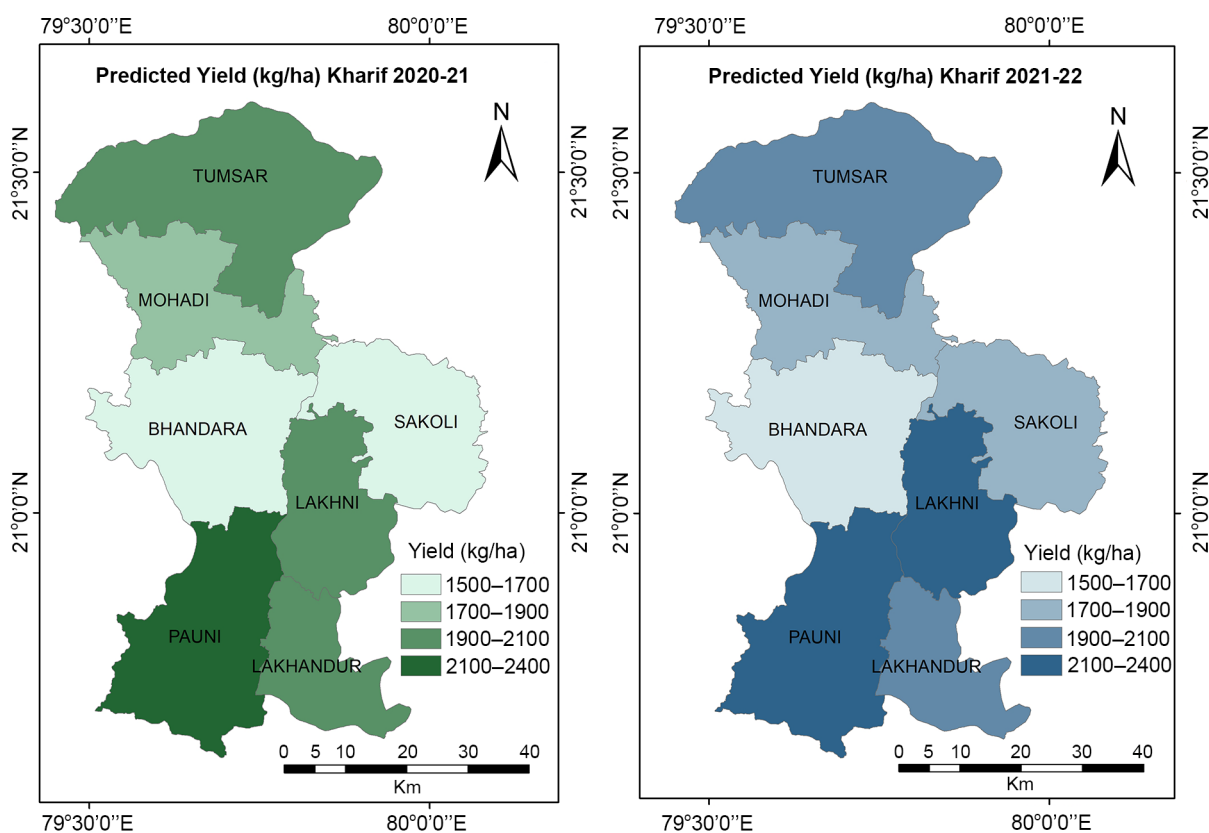
Fig. 7. Kharif rice predicted yield map (2020–2021 and 2021–2022) (source: Authors' own elaboration)

mation errors of 8–12%. Water and temperature stress parameters are critical for effectively simulating crop growth under different environmental circumstances. Similarly, studies have shown that incorporating water and temperature stress to account for non-ideal growing conditions improves yield estimation accuracy by 5–10%. It may be advantageous to fine-tune the stress indices' calibration and add additional localized data in order to reduce the yield estimates, due to reported positive bias. Deep learning and other advanced machine learning approaches have the potential to improve model performance by identifying more intricate patterns in the data. A more comprehensive understanding of the parameters that determine yield could be obtained by incorporating additional environmental variables, such as soil moisture and nutrient availability.

Multi-year studies and expanding the geographical area can assist evaluate the model under a variety of conditions and increase its robustness. Furthermore, studying the effects of climate change on yield variability would provide useful information for future agricultural planning.

CONCLUSION

In kharif rice classification, research demonstrates the successful classification of paddy crops utilizing Sentinel-1 Synthetic Aperture Radar backscatter satellite data with remarkable accuracies of 83% and 86% in the consecutive kharif seasons of 2020 and 2021, respectively. The utilization of cloud-based Google Earth Engine facilitated the efficient retrieval of Sentinel-1 SAR data, while the Random Forest classifier embedded within SNAP software proved to be an effective tool for classification purposes.

The achieved accuracies underscore the potential of SAR backscatter data in delineating paddy crop areas, crucial for agricultural monitoring and management. This methodology offers a robust and cost-effective means to monitor paddy cultivation patterns

over large geographical areas, aiding policymakers, agronomists, and stakeholders in making informed decisions regarding crop management, resource allocation, and food security strategies.

Furthermore, the consistency in accuracy across two successive seasons highlights the reliability and stability of the proposed approach, showcasing its suitability for longitudinal agricultural monitoring. The integration of advanced satellite remote sensing technologies with machine learning algorithms opens avenues for enhancing agricultural monitoring systems, enabling timely and accurate assessments of crop dynamics and land use changes.

Future research endeavors could focus on refining the classification framework by incorporating multi-temporal SAR data, exploring additional machine learning algorithms, and integrating ancillary data sources to further improve classification accuracies. Additionally, extending the analysis to encompass diverse crop types and geographical regions would enrich the applicability and generalizability of the proposed methodology, fostering advancements in precision agriculture and sustainable land management practices.

The model's foundation for yield estimation is the Monteith (1977) spectral yield estimating technique, which is used to calculate the primary net productivity of the kharif rice crop in the Bhandara district. The results of this investigation showed that crop production is dependent on the amount of photo synthetically active radiation absorbed. An additional crucial indicator for estimating the crop's net productivity is the harvest index (HI) and the product of radiation uses efficiency (RUE). The study's findings showed that the district-level paddy yield could be predicted using the said model. It is recommended that the model be improved by using radiation use efficiency values, harvest index, and geographical planting dates derived from remote sensing. With these enhancements, yield estimation at the revenue circle level will be possible, and harvest index values will be derived using field data. It contributes to the resolution of the state's crop insurance yield discrepancies.

REFERENCES

Bala, S.K.., Islam, A.S. (2009). Correlation between potato yield and MODIS-derived vegetation indices. International Journal of Remote Sensing, 30 (10), 2491–507.

Belgiu, M., Csillik, O. (2018). Sentinel-2 cropland mapping using pixel-based and object-based time-weighted dynamic time warping analysis. Remote Sensing of Environment, 204, 509–523. DOI: 10.1016/j.rse.2017.10.005

Bhattacharyya, P., Pathak, H., Pal, S. (2020). Climate smart agriculture: Concepts, challenges, and opportunities. Singapore: Springer. DOI: 10.1007/978-981-15-9132-7

Chaurasiya, G., Saxena, S., Tripathy, R., Chaudhari, K.N., Ray, S.S. (2017). Semi physical approach for sugarcane yield modelling with remotely sensed inputs. Vayu Mandal, 43(1), 11–22.

Chen, J., Lin, H., Pei, Z. (2007). Application of ENVISAT ASAR data in mapping rice crop growth in southern China. IEEE Geoscience and Remote Sensing Letters, 4 (3), 431–435. DOI: 10.1109/ LGRS.2007.896996

Chen, F., Son, R., Chang, Y., Chiang, H. (2016). Rice crop mapping using Sentinel 1A phenological metrics. Remote Sensing, XLI-B8. DOI: 10.5194/isprsarchives-XLI-B8- 863-2016

Choudhury, I., Chakraborty, M. (2006). SAR signature investigation of rice crop using RADARSAT Data. International Journal of Remote Sensing, 27 (3), 519–534. DOI: 10.1080/ 01431160500239172

Danoedoro, P. (2012). Introduction of digital remote sensing. Yogyakarta: Andi Offset.

Gummadi, S., Dinku, T., Shirsath, P.B., et al. (2022). Evaluation of multiple satellite precipitation products for rainfed maize production systems over Vietnam. Scientific Reports, 12, 485. DOI: 10.1038/s41598-021-04380-8

Klisch, A., Royer, A., Lazar, C., Baruth, B., Genovese, G. (2006). Extraction of phenological parameters from temporally smoothed vegetation indices. Methods, 3 (4), 5.

Kosmowski, F., Chamberlin, J., Ayalew, H., Sida, T., Abay, K., Craufurd, P. (2021). How accurate are yield estimates from crop cuts? Evidence from smallholder maize farms in Ethiopia, Food Policy, 102, 102122. DOI: 10.1016/ j.foodpol.2021.102122

Kumar, P.P., Sairam, M., Shankar, T., Praharaj, S., Maitra, S. (2021). Application of remote sensing in agriculture. Indian Journal of Natural Sciences, 12 (69), 37475–37479.

Lin, Y., Hu, R., Zhang, C., Chen, K. (2022). The role of public agricultural extension services in driving fertilizer use in rice production in China. Ecological Economics, 200, 107513. DOI: 10.1016/j.ecolecon.2022.107513

Ma, R., Ban, J., Wang, Q., Zhang, Y., Yang, Y., He, M.Z., Li, S., Shi, W., Li, T. (2017). Random forest model based fine scale spatiotemporal O_3 trends in the Beijing-Tianjin-Hebei region in China, 2010 to 2017. Environmental Pollution, 276, 116635. DOI: 10.1016/ j.envpol.2021.116635

Magidi, J., Nhamo, L., Mpandeli, S., Mabhaudhi, T. (2021). Application of the random forest classifier to map irrigated areas using Google Earth engine. Remote Sensing, 13 (5), 876. DOI: 10.3390/rs13050876

Mani, J.K., Varghese, A.O. (2018). Remote sensing and GIS in agriculture and forest resource monitoring. In: G.P. Obi Reddy, S.K. Singh (Eds.), Geospatial Technologies in Land Resources Mapping, Monitoring and Management, 377–400. Switzerland: Springer Nature.

Mansaray, R., Lamin, Z., Zhen, Z., Jingfeng, H. (2017). Evaluating the potential of temporal Sentinel-1A data for paddy rice discrimination at local scales. Remote Sensing Letters, 8, 10, 967–976. DOI: 10.1080/2150704X.2017.1331472

Meshram, P., Ray, S.S. (2021). Field-level crop classification using an optimal dataset of multi-temporal Sentinel-1 and polarimetric RADARSAT-2 SAR data with machine learning algorithms. Journal of the Indian Society of Remote Sensing, 49 (2), 1–14.

Meshram, P., Rawat, K.S. (2023). Detection of paddy fields in Maharashtra's eastern region during the kharif season using Sentinel-1A SAR data and geographic information system (GIS). International Conference on Advancement in Computation & Computer Technologies (InCACCT). DOI: 10.1109/InCACCT57535.2023.10141834

Monteith, J.L. (1977). Climate and efficiency of crop production in Britain. Philosophical Transactions of the Royal Society London B, 281, 277–294. DOI: 10.1098/rstb.1977.0140

Nguyen, B., Wagner, W. (2017). European rice cropland mapping with Sentinel 1 data: The Mediterranian region case study. Water, 9, 392. DOI: 10.3390/w9060392

Safdary, R., Soffianian, A., Pourmanafi, S. (2022). Application of landscape metrics and object-oriented remote sensing to detect the spatial arrangement of agricultural land. Quaestiones Geographicae, 41 (1), 25–35. DOI: 10.2478/quageo-2022-0002

Sang, H., Zhang, J., Lin, H., Zhai, L. (2014). Multi polarization ASAR backscattering from herbaceous wetland on Poyang Lake Region, China. Remote Sensing, 6, 4621–4646. DOI: 10.3390/rs6054621

Schubert, A., Small, D., Miranda, N., Geudtner, D., Meier, E. (2015). Sentinel-1A product geolocation accuracy: Commissioning phase results. Remote Sensing, 7 (7), 9431–9449. DOI: 10.3390/rs70709431

Silveira, E.M.O., Silva, S.H.G., Acerbi-Junior, F.W., Carvalho, M.C., Carvalho, L.M.T., Scolforo, J.R.S., Wulder, M.A. (2019). Object-based random forest modelling of aboveground forest biomass outperforms a pixel-based approach in a heterogeneous and mountain tropical environment. International Journal of Applied Earth Observation and Geoinformation, 78, 175–188. DOI: 10.1016/j.jag.2019.02.004

Son, N.T., Chen, C.F., Chen, C.R., Minh, V.Q., Trung, N.H. (2014). A comparative analysis of multitemporal MODIS EVI and NDVI data for large-scale rice yield estimation. Agricultural and Forest Meteorology, 197, 52–64. DOI: 10.1016/j.agrformet.2014.06.007

Subbarao, N.V.V.S.S.T., Mani, J.K., Shrivastava, A., Srinivas, K., Varghese, A.O. (2020). Acreage estimation of kharif rice crop using Sentinel-1 temporal SAR data. Spatial Information Research, 29. DOI: 10.1007/s41324-020-00374-2

Tikkiwal, G.C., Alka Khandelwal (2012). Crop acreage and crop production estimates for small domains – revisited. Statistics in Transition, new series, 13, 1, 47–64. DOI: 10.59170/stattrans-2012-004

Torre dela, D.M.G., Gao, J., Macinnis-Ng, C. (2021). Remote sensing-based estimation of rice yields using various models: A critical review. Geo-Spatial Information Science, 24 (4), 580–603. DOI: 10.1080/10095020.2021.1936656 DOI: 10.1007/s12524-021-01436

United Nations (UN). The Sustainable Development Goals Report (2021). https://unstats.un.org/sdgs/report/2021/The-Sustainable-Development-Goals-Report-2021.pdf (accessed: September 23, 2024).

Valcarce-Diñeiro, R., Arias-Pérez, B., Lopez-Sanchez, J.M., Sánchez, N. (2019). Multi-temporal dual- and quad-polarimetric synthetic aperture radar data for crop-type mapping. remote sensing, 11 (13), 1518. DOI: 10.3390/rs11131518

Xiao, X., Hollingerb, D., Abera, J., Goltzc, M., Davidsond, E.A., Zhanga, Q. (2004). Satellite-based modeling of gross primary production in an evergreen needle leaf forest. Remote Sensing of Environment, 89, 519–534.

SZACOWANIE POWIERZCHNI UPRAW I PLONÓW RYŻU SEZONU MONSUNOWEGO (CHARIF) PRZY UŻYCIU SZEREGU CZASOWEGO DANYCH SATELITARNYCH Z TELEDETEKCJI MIKROFALOWEJ I OPTYCZNEJ: STUDIUM PRZYPADKU WSCHODNIEGO REGIONU MAHARASZTRA

ABSTRAKT

Cel pracy
Badanie ma na celu ocenę wykonalności wykorzystania teledetekcji do oszacowania powierzchni upraw oraz plonów w głównym regionie uprawy ryżu w regionie Maharasztra.

Materiał i metody
Ostatnie postępy w technologii teledetekcji, w tym poprawa rozdzielczości i dostępności obrazu, umożliwiają szybkie i terminowe zbieranie danych. Badanie wykorzystuje losowy klasyfikator lasu do identyfikacji upraw ryżu przy użyciu czasowych obrazów wstecznego rozpraszania SAR Sentinel-1A. Ponadto do oszacowania plonów stosuje się metodę z pogranicza fizyki, która łączy techniki oparte na teledetekcji i na fizjologii roślin, takie jak promieniowanie fotosyntetycznie czynne oraz ułamek PAR pochłoniętego przez uprawę.

Wyniki i wnioski
Produkt pierwotny netto oblicza się przy użyciu modelu Monteitha. Plony ryżu z uprawy charif obliczono, biorąc pod uwagę rzeczywisty NPP, efektywność wykorzystania promieniowania oraz indeks zbiorów. Badania prowadzono na przestrzeni dwóch sezonów charif, w 2020 i 2021 roku. Chociaż zanotowano (niewielkie) różnice, zarówno w odniesieniu do powierzchni ryżu z uprawy charif, jak i w szacunkach plonów, model ten nadal jest skuteczny i odpowiedni do zastosowania w innych znaczących regionach uprawy ryżu charif w kraju.

Słowa kluczowe: teledetekcja, NPP, temperatura, FAPAR, LSWI